In situ Characterization of Photoresist Dissolution

Toshiro Itani and Julius Joseph Santillan

Semiconductor Leading Edge Technologies Inc., 16-1 Onogawa, Tsukuba, Ibaraki 305-8569, Japan

Received April 23, 2010; accepted May 14, 2010; published online June 4, 2010

The dissolution process plays an important role in optimizing photoresist materials and processes for next-generation lithographic technologies. In this paper, we describe the application of high-speed atomic force microscopy for *in situ* analysis and characterization of photoresist dissolution. In particular, the physical changes in an exposed extreme ultraviolet (EUV) photoresist film are analyzed in real time—before, during, and after the development process. In this initial work, we report the dissolution characteristics of an EUV-exposed poly(4-hyrdroxystyrene)-based polymer resist processed with a tetramethylammonium hydroxide developer solution.

DOI: 10.1143/APEX.3.061601

Extreme ultraviolet (EUV) photoresist materials and processing are considered as one of the most critical issues in achieving the desired targets for EUV lithography.[1–4] Extensive research has been conducted on high-performance photoresist materials,[2–12] and recently numerous improved methods for photoresist processing have been reported.[13–16] Photoresist development or dissolution is one such process that has been extensively studied,[17–22] and it has garnered increasing attention over the past few years.[13,14,16,23]

Various analysis methods, such as the quartz crystal microbalance[24,25] and dissolution rate monitors,[26,27] provide information that can help describe or define the behavior of a photoresist film during the dissolution process. However, until now there has been no direct evidence of the mechanism operational on the photoresist film during this chemical process. A visual observation of the actual pattern formation of photoresists during dissolution may provide new pointers concerning further improvement of the performance of the photoresist process.

Research on atomic force microscopy (AFM) has led to the development of ultra-fast scanning and nano-level analysis capabilities over the years. AFM measurements performed under a liquid solution have also improved and are already being applied in the dynamic observation of biomolecular processes.[28] These continuous improvements in AFM capabilities indicate a remarkable potential in its application for the *in situ* analysis of the dissolution behavior of a photoresist.

Figure 1 shows a picture of the high speed AFM (HS-AFM) system (Nano Live Vision by Research Institute of Biomolecule Metrology), which is used here in the intermittent-contact mode. The HS-AFM system comprises a "sample assembly" to which a resist-coated and EUV-exposed wafer sample is attached and a "cantilever assembly" where the cantilever and developer solution are set. An extensively improved version of the AFM reported in an earlier paper,[28] the HS-AFM is equipped with highly sensitive, ultra-fast cantilever, and AFM scanning capabilities (temporal resolution: 80 ms/image).

The cantilever has a resonance frequency of approximately 1 MHz in water and a spring constant of 0.1–0.3 N/m. An amorphous carbon tip was grown on the original cantilever tip by electron beam deposition. The tip length was adjusted to about 1 μm, and the tip apex was sharpened by plasma etching (<15 nm in radius). A deflection sensor is focused onto a small cantilever with an objective lens (20 times magnification). For the analysis, an approximately

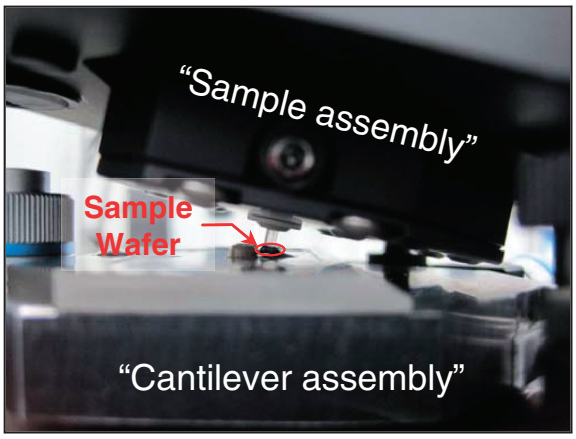

Fig. 1. A picture of HS-AFM system (RIBM Nano Live Vision) used here in intermittent-contact mode.

$2 \times 2\,mm^2$ wafer sample is set on a sample stage made of quartz glass. All HS-AFM measurements were performed at room temperatures.

For these initial analyses, an EUV positive-tone poly(4-hyrdroxystyrene)-based polymer resist, the Selete standard resist 5 (SSR5) was utilized at a film thickness of 60 nm.[13,14] The post-application bake was at a temperature of 120 °C for 90 s, while the post-exposure bake was at 100 °C for 90 s.[13,14] A 0.26 N tetramethylammonium hydroxide (TMAH) developer solution was utilized at a 1/20 diluted concentration to reduce the development speed and thus allow a clearer analysis of the dynamic development process.

The wafer samples were prepared using the small field exposure tool (SFET, numerical aperture = 0.3).[2,13,14] The SFET was linked to a coater/developer track system (Tokyo Electron Clean track ACT12) in a chemically controlled environment. The standard illumination condition used for the evaluation of the photoresist materials was an annular illumination of σ_{outer} 0.7/σ_{inner} 0.3. The 32-nm isolated line (I/L) pattern exposures were made on a 300-mm φ silicon wafer, which was then cleaved to obtain the $2 \times 2\,mm^2$ wafer samples used for the *in situ* analysis. To obtain reference images of the SSR5 under standard photoresist processes, S-9380II (Hitachi High-Technologies) scanning electron microscope (SEM) for the top view and S5000 (Hitachi High-Technologies) for the cross-section view was utilized at optimal conditions.[13]

Figure 2 shows the process flow of the preparation for HS-AFM analysis. First, the assembly and setup of the "cantilever assembly" and "sample assembly" were per-

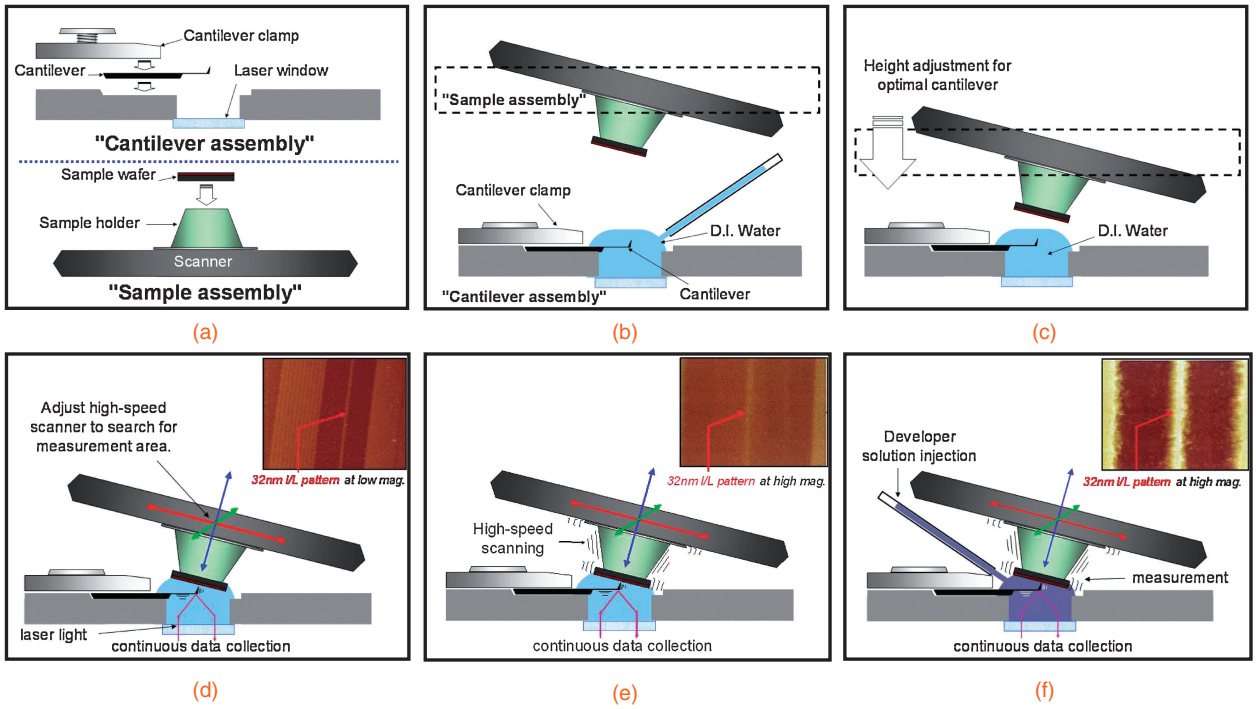

Fig. 2. The process flow in the preparation for HS-AFM analysis.

formed (a). Next, a pre-determined volume of de-ionized (DI) water was injected onto the cantilever assembly (b), after which the sample assembly was adjusted to the optimal distance from the cantilever assembly (c). Data collection or roughness information, obtained by observing the variation of the laser reflected from the oscillating cantilever, begins while adjusting the high-speed AFM scanner's x, y, and z values to position the cantilever on measurement area (d). High-speed scanning is performed to evaluate the initial surface conditions of the sample wafer before the development process (e). During the AFM high-speed scanning, a predetermined volume of developer solution was injected and the scanning was continued until dissolution was completed (f).

Figure 3 shows the top view of the development of the 32-nm I/L pattern exposed on the SSR5 at a series of arbitrary points of time (t0–t10). As a reference, the top view obtained by an SEM after a standard photoresist process is also shown.

It can be observed that at time 0 (t0), with the photoresist film analyzed under DI water, some thickness loss assumed to be due to EUV exposure already exists. As the 0.26 N TMAH developer solution was injected into the DI water, resulting in a 1/20 concentration, the developing process began and was observed as an increase in film roughness at t1 and t2 of the EUV-exposed area on both sides of the 32-nm I/L pattern. The variation in roughness of the exposed area increases at t3, where some dark spots among the resist grains (representing generated pits) start to appear, indicating the disintegration or dissolution of the exposed photoresist film. The dissolution continues from t4 to t7, where the 32-nm I/L pattern starts to manifest. The dissolution continues after t7 until only the 32-nm I/L pattern remains, and the development process is assumed to finish at t10.

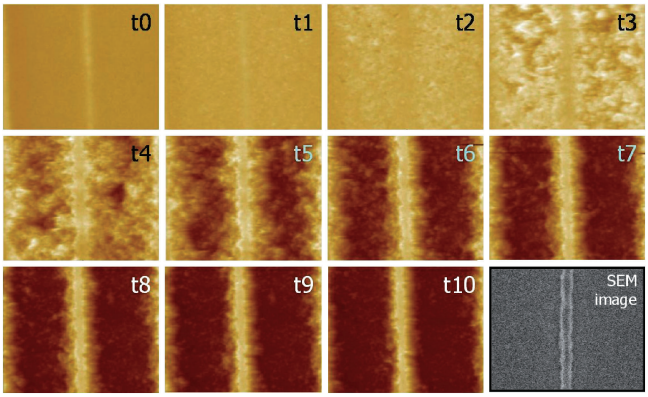

Fig. 3. Top view of the 32-nm I/L pattern exposed on SSR5 at increasing development times (t0–t10). As a reference, a top-view SEM image obtained after a standard photoresist process is also shown.

Figure 4 shows the *in situ* development analysis results of the 32-nm I/L pattern exposed on SSR5 after a three-dimensional (3D) rendering. As a reference, a cross-sectional SEM image obtained after a standard photoresist process is also shown.

These results provide a direct visual representation of the actual dissolution process. From t4, large areas of the EUV-exposed film begin to dissolve rapidly, and by t8 only a few sections on both sides of the 32-nm I/L continue to dissolve. Note that at t4 some resist swelling (an increase in film roughness beyond the original resist thickness) occurs, but immediately disappears at t5. Moreover, upon a finer analysis of the 3D results at t5 and beyond, a consistent swelling can be observed directly on the top edges of the 32-nm I/L pattern. This swollen film was especially prominent at t6, and it continued to remain even until t10 where the dissolution process is assumed to have finished. This

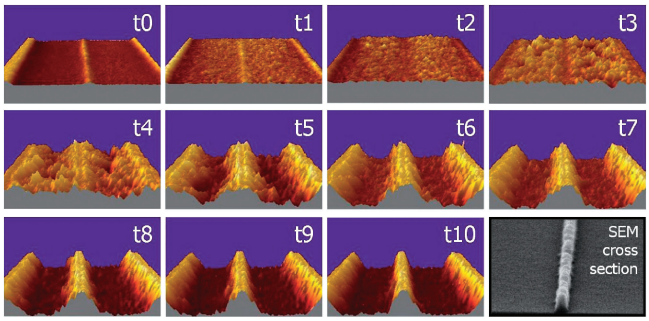

Fig. 4. The 32-nm I/L pattern exposed on SSR5 after 3D rendering. As reference, a cross-sectional SEM image obtained after a standard photoresist process is also shown.

phenomenon at the edge of the pattern provides possible pointers for explaining the mechanism of the effect of the development process on the line width roughness. However, further work is necessary for better comprehension of the mechanism.

In summary, we conducted an *in situ* analysis of photoresist dissolution using the HS-AFM. These initial results indicated the potential of this method and provided new insights into the actual dissolution process of photoresists. Moreover, the results supported numerous previous assumptions about photoresist dissolution mechanisms and presented possible pointers that may help in the understanding and advancement of photoresists for use in next-generation applications.

Acknowledgments A part of this work was supported by the New Energy and Industrial Technology Development Organization (NEDO). We would like to thank Selete member companies (EUV Lithomask program) for their continued support and photoresist and material manufacturers for providing the latest photoresist technologies.

1) International Technology Roadmap for Semiconductors 2009 Edition, Lithography.
2) H. Oizumi, K. Matsumaro, J. Santillan, G. Shiraishi, K. Kaneyama, K. Matsunaga, and T. Itani: Proc. SPIE **7639** (2010) 76390R.
3) R. Lawson, J. Cheng, D. Noga, T. Younkin, L. Tolbert, and C. Henderson: Proc. SPIE **7639** (2010) 76390O.
4) C. Koh, J. Georger, L. Ren, G. Huang, F. Goodwin, S. Wurm, D. Ashworth, W. Montgomery, B. Pierson, J. Park, and P. Naulleau: Proc. SPIE **7636** (2010) 763604.
5) R. Allen, P. Brock, Y.-H. Na, M. Sherwood, H. Truong, G. Wallraff, M. Fujiwara, and K. Maeda: J. Photopolym. Sci. Technol. **22** (2009) 25.
6) T. Itani, H. Oizumi, K. Kaneyama, D. Kawamura, S. Kobayashi, and J. J. Santillan: J. Photopolym. Sci. Technol. **22** (2009) 59.
7) C. Higgins, A. Antohe, G. Denbeaux, S. Kruger, J. Georger, and R. Brainard: Proc. SPIE **7271** (2009) 727147.
8) M. Shirai, K. Maki, H. Okamura, K. Kaneyama, and T. Itani: J. Photopolym. Sci. Technol. **22** (2009) 111.
9) T. Nishikubo, H. Kudo, Y. Suyame, H. Oizumi, and T. Itani: J. Photopolym. Sci. Technol. **22** (2009) 73.
10) M. Wang, C. T. Lee, C. Henderson, W. Yueh, J. M. Roberts, and K. Gonsalves: Proc. SPIE **6923** (2008) 692312.
11) H. Oizumi, T. Kumise, and T. Itani: J. Vac. Sci. Technol. B **26** (2008) 2252.
12) T. Watanabe and H. Kinoshita: J. Photopolym. Sci. Technol. **20** (2007) 373.
13) K. Matsunaga, H. Oizumi, K. Kaneyama, G. Shiraishi, K. Matsumaro, J. J. Santillan, and T. Itani: Proc. SPIE **7636** (2010) 76360S.
14) K. Kaneyama, K. Matsunaga, G. Shiraishi, J. J. Santillan, and T. Itani: Proc. SPIE **7636** (2010) 763633.
15) N. Bradon, K. Nafus, H. Shite, J. Kitano, H. Kosugi, M. Goethals, S. Cheng, J. Hermans, E. Hendrickx, B. Baudemprez, and D. Van Den Heuvel: Proc. SPIE **7636** (2010) 763630.
16) S. Putna, T. Younkin, R. Caudillo, and M. Chandhok: Proc. SPIE **7636** (2010) 76360P.
17) T. Itani, H. Iwasaki, M. Fujimoto, and K. Kasama: Jpn. J. Appl. Phys. **33** (1994) 7005.
18) T. Itani, H. Yoshino, S. Hashimoto, M. Yamana, N. Samoto, and K. Kasama: J. Vac. Sci. Technol. B **15** (1997) 2541.
19) T. Itani, S. Hashimoto, M. Yamana, N. Samoto, and K. Kasama: Microelectron. Eng. **41–42** (1998) 363.
20) T. Itani, H. Yoshino, S. Hashimoto, M. Yamana, M. Miyasaka, and H. Tanabe: J. Vac. Sci. Technol. B **16** (1998) 3726.
21) T. Kodani, T. Ishikawa, T. Yoshida, T. Hayami, M. Koh, T. Moriya, T. Yamashita, M. Toriumi, T. Araki, H. Aoyama, T. Hagiwara, T. Furukawa, T. Itani, and K. Fujii: J. Vac. Sci. Technol. B **22** (2004) 3509.
22) T. Itani, K. Kaneyama, T. Kozawa, and S. Tagawa: J. Vac. Sci. Technol. B **26** (2008) 2261.
23) T. Itani and J. J. Santillan: J. Vac. Sci. Technol. B **27** (2009) 2986.
24) W. Hinsberg, F. Houle, S.-W. Lee, H. Ito, and K. Kanazawa: Macromolecules **38** (2005) 1882.
25) M. Toriumi, J. Santillan, T. Itani, T. Kozawa, and S. Tagawa: J. Vac. Sci. Technol. B **25** (2007) 2486.
26) A. Kokkinis, E. S. Valamontes, and I. Raptis: J. Phys.: Conf. Ser. **10** (2005) 401.
27) A. Agrawal and C. L. Henderson: Proc. SPIE **5038** (2003) 1026.
28) T. Ando, T. Uchihashi, N. Kodera, D. Yamamoto, A. Miyagi, M. Taniguchi, and H. Yamashita: Pflugers Arch. **456** (2008) 211.